Looped Manifold Trajectories of Dynamic Functional Connectivity Reveal Continuous Task-related Brain Reconfiguration

Yueran Li[1], Xinle Chang[1], Yang Yang[1], Chenfei Ye[1], Yu Zhao[2] & Jingyong Su (sujingyong@hit.edu.cn) *[1]
[1]School of Computer Science and Technology, Harbin Institute of Technology (Shenzhen)
[2]Department of Radiology, Huaxi MR Research Center (HMRRC), Institute of Radiology and Medical Imaging, West China Hospital of Sichuan University

Abstract

Dynamic functional connectivity (dFC) matrices capture time-varying interactions among large-scale brain networks, but their high spatiotemporal dimensionality complicates the interpretation of how whole-brain functional organization is configured and reconfigured across cognitive tasks. In this work, we introduce a geometric framework that embeds sliding-window dFC from resting-state and task fMRI into a shared low-dimensional manifold. Within this space, resting-state dFC embeddings cluster within a compact intrinsic resting-state region of the manifold that serves as a functional baseline, whereas task engagement yields smooth, looped trajectories that depart from and return to this baseline. Distinct tasks trace separable loop structures that remain stable across parcellation resolutions. Phase-dependent sampling of dFC matrices along these loops reveals structured, time-ordered reconfigurations of functional networks during task performance. Together, these findings depict brain dynamics as continuous, recurrent trajectories rather than discrete state transitions, providing a unified geometric representation of task-evoked dynamic functional reconfiguration.

Keywords: Manifold Learning, fMRI, Dynamic Functional Connectivity, Isomap

Introduction

Functional Magnetic Resonance Imaging (fMRI), by measuring the blood-oxygen-level-dependent (BOLD) signal, has become a cornerstone technique for mapping the functional organization of the human brain (Biswal et al., 1995; Logothetis, 2008). A central goal of fMRI research is to move beyond localized activations and characterize how distributed brain regions coordinate as coherent networks to support cognition and behavior. To achieve this goal, functional connectivity (FC) quantifies inter-regional statistical dependencies in BOLD activity, providing a network-level description of large-scale functional organization. Traditional FC analyses typically assume stationarity of these dependencies over the scan duration. Yet converging evidence indicates that functional interactions evolve continuously, with large-scale networks reconfiguring to meet changing cognitive demands (Allen et al., 2014; Hutchison et al., 2013). Therefore, dynamic functional connectivity (dFC) methods have been increasingly adopted to track these time-varying coupling patterns (Cohen, 2018; Lurie et al., 2020; Preti et al., 2017).

Despite the descriptive richness of dFC matrices, their high spatiotemporal dimensionality poses a fundamental interpretability challenge. Even with a moderate parcellation, each windowed dFC matrix is a point in a high-dimensional space, and the dFC sequence traces a complex trajectory that is hard to visualize. To deal with this complexity, many studies adopt discrete-state summaries by clustering windowed connectivity patterns (e.g., k-means) or using related state-space models (Allen et al., 2014; Vidaurre et al., 2017). However, such discretization may blur smooth temporal functional evolution and inter-pattern geometry, potentially masking continuous, recurrent task-related reconfiguration.

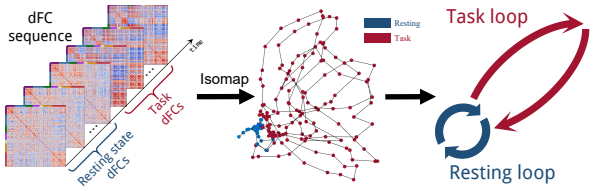

Figure 1: Dynamic functional connectivity (dFC) matrices embedded with Isomap form looped trajectories with a compact resting loop and a larger task loop.

Recent advances, inspired by the manifold hypothesis, propose that while the dimensionality of the measurement space (number of voxels or edges) is high, the intrinsic degrees of freedom governing neural dynamics are relatively low (Gallego et al., 2017; Shine et al., 2019). According to this view, brain dynamics evolve along a low-dimensional manifold (a curved geometric structure embedded within the high-dimensional signal space), where trajectories represent the temporal evolution of brain network configurations (Perl et al., 2025; Roberts et al., 2019).

To recover the intrinsic geometry of high-dimensional dFC, nonlinear manifold learning offers clear advantages over linear projections by preserving local neighborhood structure and nonlinear variation. Such techniques have been widely used to map macroscale gradients of cortical organization (Margulies et al., 2016) and to reveal low-dimensional neural trajectories during cognition (Busch et al., 2023; Shine et al., 2019). Importantly, manifold-based dFC studies either embed windowed or time-resolved connectivity into a low-dimensional space and then apply clustering or state-space summaries to identify recurring states or coupling motifs (Gao et al., 2020; Huang et al., 2021; Yang et al., 2019), or compute matrix-wise connectivity gradients and cluster these summaries to capture

*Corresponding author

In G. Boleda, I. Dautriche, M. Maldonado, C. Saldana and T. Torrent (Eds.), *Proceedings of the 48th Annual Conference of the Cognitive Science Society*

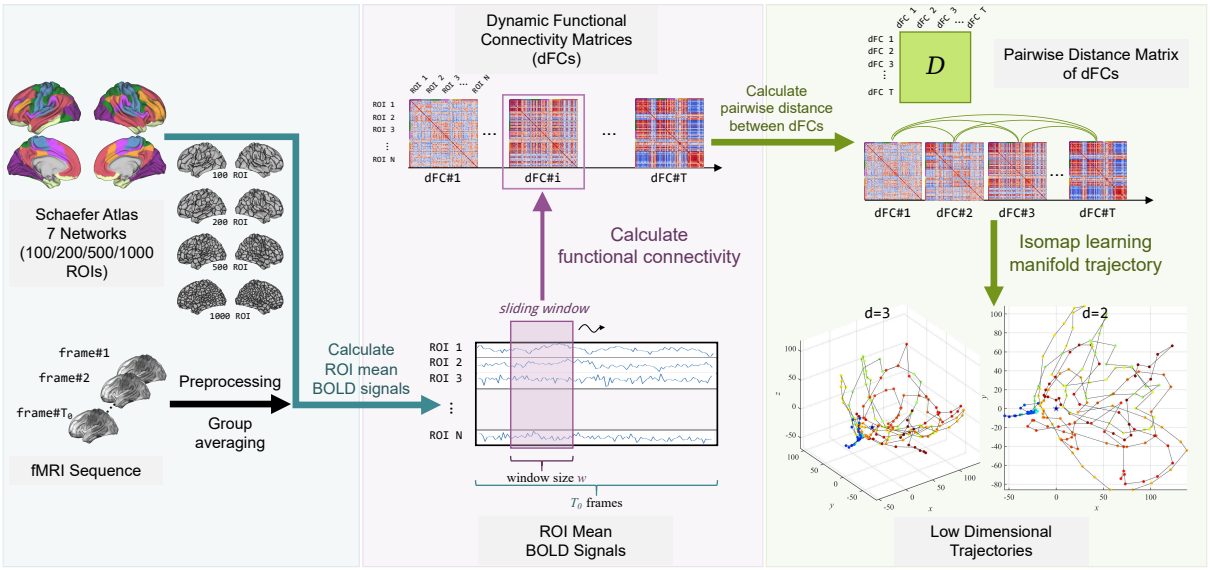

Figure 2: The framework of the proposed dFC manifold learning pipeline.

within-matrix modular or state-like structure (Soleimani et al., 2025). However, most existing studies either analyze resting-state and task-evoked dynamics in isolation, or ultimately reduce dFC to discrete state transitions, so the global geometric relationship between the intrinsic resting baseline and task-driven reconfiguration has not been systematically characterized within a unified geometric framework (Rué-Queralt et al., 2021).

In this study, we propose a unified manifold-learning framework that represents whole-brain functional reconfiguration as continuous trajectories in a shared low-dimensional space. We embed sliding-window dFC sequences from resting-state and task fMRI (Emotion and Motor) into a common manifold using Isomap (Tenenbaum et al., 2000). This approach follows the manifold hypothesis: dFC patterns lie near a low-dimensional manifold embedded in a high-dimensional space, and Isomap approximates the manifold's geodesic distances by stitching together local Euclidean neighborhoods through shortest paths on a neighborhood graph. In the resulting manifold space, resting-state dFCs concentrate near a compact baseline region, whereas task engagement produces smooth, task-specific departures that form looped trajectories returning toward baseline as Figure 1 shows, enabling direct geometric comparison across cognitive contexts within an integrated manifold representation.

In summary, this work makes three main contributions. First, we embed resting-state and task-evoked dFC into a shared manifold, establishing an intrinsic resting baseline and placing task-driven reconfiguration in the same geometric coordinate system rather than treating rest and task as separate regimes. Second, we model task engagement as smooth, often looped trajectories that depart from and return to this baseline, capturing continuous and recurrent brain functional reconfiguration beyond discrete states. Third, by using loop phase to index dFC sampling along the manifold, we uncover a reproducible, ordered sequence of large-scale coupling reconfigurations that unfolds continuously around an outward–return cycle, providing an interpretable alternative to discrete state descriptions.

Method

To characterize the intrinsic geometric structure of dynamic brain states, we propose a nonlinear manifold-learning framework for dFCs. We represent whole-brain activity with region-of-interest (ROI) mean time series derived from cortical parcellation, and compute sliding-window dFC from these ROI mean signals. The analytic pipeline is illustrated in Figure 2.

ROI Mean BOLD Signals Calculation

Following the standard preprocessing pipeline, we averaged resting-state and task fMRI time series across subjects to obtain group-mean signals. This step attenuates individual-specific noise and highlights cohort-consistent dynamics. We then extracted ROI-wise mean BOLD time series using the **Schaefer atlas** (Schaefer et al., 2018), which is derived from a gradient-weighted Markov Random Field model and hierarchically aligned to the Yeo 7-network parcellation (Yeo et al., 2011). To assess robustness across spatial scales, we repeated all analyses at four parcellation resolutions, $N \in \{100, 200, 500, 1000\}$, where N denotes the number of whole-brain ROIs defined by the parcellation. This yielded an ROI-wise time series matrix $X \in \mathbb{R}^{N \times T_0}$, where T_0 denotes the total number of temporal frames in the fMRI sequence. To mitigate T1-equilibration effects and ensure magnetization stability, we discarded the first $o = 5$ frames of each raw sequence.

Dynamic Functional Connectivity Construction

To quantify brain functional reconfiguration over time, we estimated dFC using the widely adopted sliding-window approach (Hutchison et al., 2013). We defined a sliding window with a length of $w = 10$ TRs and a step size of $s = 1$ TR. Given the original time series length T_0, with the first $o = 5$ frames discarded, the total number of temporal frames T in the final dFC sequence is governed by the following equation:

$$T = \left\lfloor \frac{T_0 - o - w}{s} \right\rfloor + 1. \quad (1)$$

For each time step $t \in \{1, \ldots, T\}$, we extracted a windowed signal matrix $X^{(t)} \in \mathbb{R}^{N \times w}$ from the original time series X, spanning the interval $[s(t-1)+1, s(t-1)+w]$. The dynamic functional connectivity matrix at time t, denoted as $\mathbf{C}_t \in \mathbb{R}^{N \times N}$, was computed as the Pearson correlation matrix of $X^{(t)}$. Specifically, the element (i, j) of $\mathbf{C}_t$ represents the Pearson correlation coefficient between the row vectors corresponding to ROI i and ROI j within the windowed segment $X^{(t)}$. This process yielded a temporally ordered sequence of functional connectivity matrices $C = \{\mathbf{C}_1, \mathbf{C}_2, \ldots, \mathbf{C}_T\}$, encoding the instantaneous functional architecture of the brain.

Isomap Embedding of dFC into a Shared Manifold

The core of our approach involves mapping the high-dimensional sequence of connectivity matrices onto a low-dimensional manifold to reveal the underlying state-space trajectory. We treated each connectivity matrix $\mathbf{C}_t$ as a discrete point in a high-dimensional feature space.

We computed a pairwise distance matrix $D \in \mathbb{R}^{T \times T}$ representing the dissimilarity between brain states at different time points. The distance between two functional connectivity states t_i and t_j was defined as the Frobenius norm of the difference between their respective correlation matrices:

$$D_{ij} = ||\mathbf{C}_{t_i} - \mathbf{C}_{t_j}||_F = \sqrt{\sum_{p=1}^{N}\sum_{q=1}^{N}\left(\mathbf{C}_{t_i}^{(p,q)} - \mathbf{C}_{t_j}^{(p,q)}\right)^2}. \quad (2)$$

To recover the intrinsic geometry of the data, we applied **Isomap** (Isometric Feature Mapping) to the distance matrix D (Tenenbaum et al., 2000). Unlike linear methods (e.g., PCA) that preserve global variance, Isomap estimates the geodesic distance along the curved manifold by constructing a k-nearest neighbor graph and finding shortest paths. This allows for the unfolding of non-linear structures. In this work, we set $k = 10$. We projected the data into a low-dimensional space ($d = 3$ or 2), yielding a set of coordinates $Y = \{y_1, y_2, \ldots, y_T\}$ that form a continuous trajectory. This trajectory visualizes the temporal evolution of whole-brain integration and segregation, revealing potential cyclic patterns or attractor dynamics (see Results).

Experiment

Dataset

The dataset was obtained from the WU-Minn Human Connectome Project Young Adult (HCP-YA) 2025 release (Van Essen et al., 2013), comprising 100 unrelated healthy adults (ages 22–35, sex-balanced) to minimize genetic confounds. Whole-brain resting-state and task fMRI were acquired on a 3T Siemens Connectome Skyra scanner using a multi-band EPI sequence (TR = 0.72 s; 2 mm isotropic voxels).

Task design

The emotion task, adapted from Hariri et al. (2002), assessed affective processing by requiring participants to match shapes or faces (expressing anger or fear). Each of the two runs comprised three 21s face blocks and two 21s shape blocks, consisting of a 3s cue followed by each trial. The motor task mapped specific motor areas following protocols by Buckner et al. (2011). Participants responded to visual cues by tapping fingers (left/right hand), squeezing toes (left/right foot), or moving their tongue. Each run contained 10 task blocks (two per condition) interleaved with three 15s fixation blocks.

Preprocessing

All fMRI data (resting-state, motor, and emotion tasks) used in this work underwent the HCP minimal preprocessing pipeline (Smith et al., 2013), including motion/distortion correction and normalization to standard CIFTI grayordinates fs_32k_LR surface. The HCP 2025 release utilized spin-echo–based ("SEBASED") bias field correction and incorporated multi-run spatial ICA-FIX (sICA+FIX), reclean, and temporal ICA pipelines (Glasser et al., 2018, 2019). Strictly adhering to HCP recommendations, we exclusively utilized the 2025 release data, avoiding any mixture with the earlier 2017 S1200 release. For subsequent analyses, we applied spa-

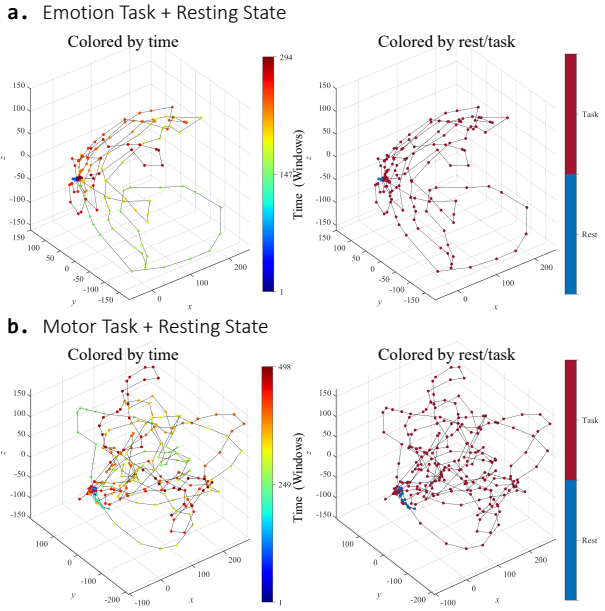

Figure 3: Low-dimensional trajectories of (a) Emotion+Rest and (b) Motor+Rest dFCs, colored by time (left) and by state (right; blue=rest, red=task)

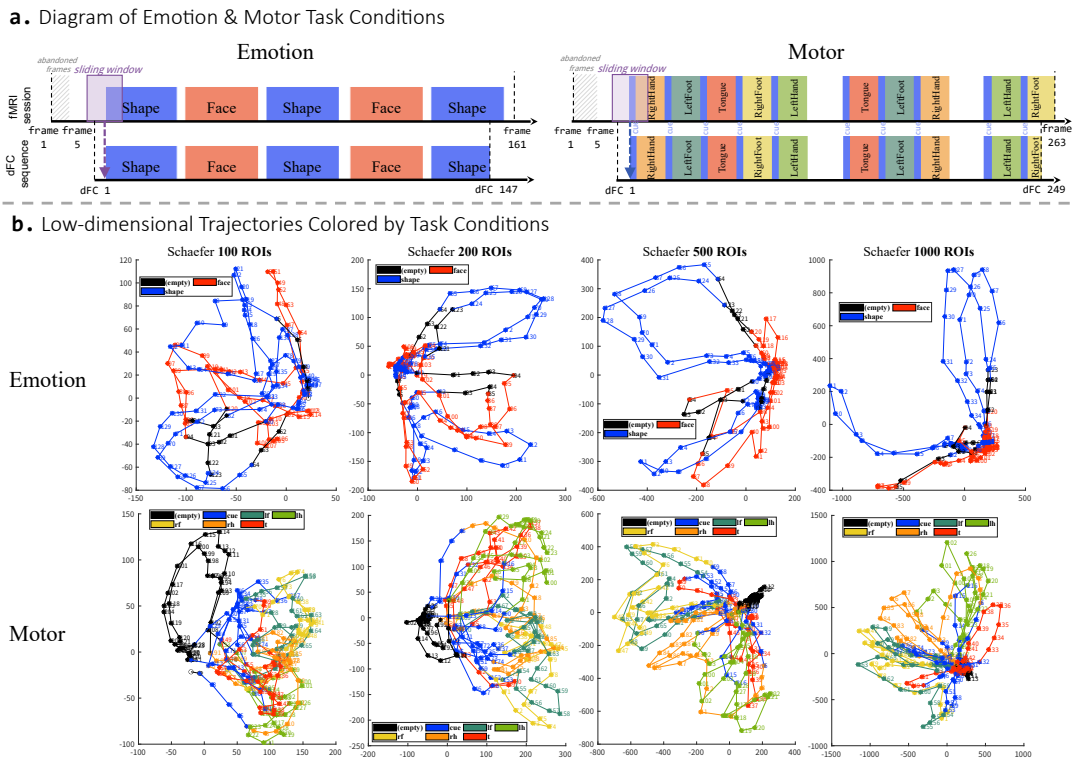

Figure 4: Task paradigms and manifold trajectories of different task dFCs. (a) Experimental design of the HCP Emotion and Motor tasks, illustrating the sequence of task blocks and corresponding dFC time indices. (b) Trajectories of dFCs calculated for four atlas resolutions (Schaefer 100, 200, 500, 1000 ROIs). Trajectories are colored by condition: face/shape (Emotion), lf/lh/rf/rh/t (Motor: left/right foot/hand, tongue), cue (visual cue), and empty (baseline).

tial smoothing (4 mm FWHM Gaussian kernel) and vertex-wise demeaning to reduce inter-individual differences.

Results

Resting and task-evoked dFC trajectories exhibit distinct geometric regimes To characterize how intrinsic and task-evoked dynamics jointly occupy a common state space, we concatenated sliding-window dFC sequences from resting-state and task fMRI and projected the combined series into a shared low-dimensional manifold using Isomap. As shown in Figure 3, within this embedding, resting-state dFC embedding points remain spatially confined, forming a dense cluster that defines a compact baseline. In contrast, task demands trigger large-scale excursions away from this baseline, with task-evoked trajectories manifesting as smooth, looped curves in the low-dimensional space. These loop-like paths reveal a clear geometric separation between intrinsic baseline activity and task-evoked regimes, indicating that task engagement drives continuous, cyclic reconfigurations of whole-brain functional connectivity rather than abrupt transitions between a small number of discrete states. This smoothness stems from sliding-window autocorrelation, which attenuates high-frequency noise to effectively reveal continuous functional network evolution.

From a manifold perspective, the resting cluster provides a functional baseline, whereas the cyclic trajectories describe the continuous modulation of network architecture during task performance (Figure 3b). Starting from this baseline, the system evolves into distinct task-specific configurations to meet cognitive demands and subsequently returns toward the resting region. These findings are consistent with established models of brain state modulation and indicate that functional dynamics can be compactly described as structured traversals along a low-dimensional manifold.

Task-condition–specific looped trajectories across parcellation resolutions To investigate whether the observed manifold trajectories capture task-specific functional signatures, we mapped the task paradigms onto the dFC embeddings. As detailed in Figure 4a, we labeled each low-dimensional point based on the task condition of the emotion (shape vs. face) and motor (right/left hand, right/left foot, tongue) tasks at the sliding window's temporal midpoint.

This visualization reveals a fine-grained segregation of functional dynamics within the task loops (Figure 4b). Rather than following a unitary, undifferentiated trajectory, different neural states diverge into distinct sub-loops corresponding to specific cognitive demands. Specifically, the emotion task trajectories bifurcate into condition-specific paths, while the

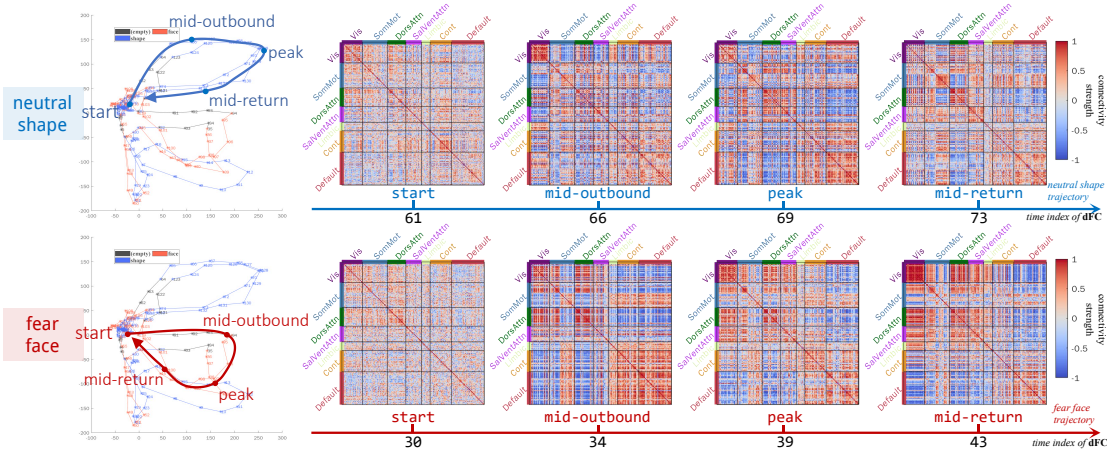

Figure 5: Looped dFC trajectories during the emotion task, with representative connectivity patterns sampled at key phases along the manifold trajectory (start, mid-outbound, peak, and mid-return).

motor task exhibits a pronounced radial, petal-like topology, where distinct motor conditions generate unique, directed excursions radiating from the central resting cluster.

Crucially, this trajectory bifurcation offers a geometric interpretation of how the brain navigates diverse cognitive states. In this framework, different tasks drive direction-specific looped trajectory, whose direction reflects task-specific network modulation and whose amplitude (the distance from the resting baseline) reflects reconfiguration magnitude.

Across parcellation scales (Schaefer 100, 200, 500, 1000 ROIs), the global topology remains robust, while finer parcellations yield more compact trajectories and sharper manifold definition. While the fundamental cyclic segregation remains invariant across all scales, finer parcellations yield noticeably more compact trajectories. This indicates that increasing spatial granularity reduces the variance within task states, thereby sharpening the definition of the manifold trajectories without altering their intrinsic topology.

Trajectory phase aligns with ordered dFC reconfiguration To elucidate the neurophysiological underpinnings of the observed trajectory loops, we extracted functional connectivity matrices corresponding to specific phases of the manifold dynamics. For each condition within both the Emotion and Motor tasks, we selected a representative trajectory loop and identified four key landmarks: Start, Mid-outbound, Peak, and Mid-return (Figure 5 left).

At the Start phase, a consistent functional architecture characterizes the baseline across all conditions. Reflecting its proximity to the resting cluster, this state exhibits a modular architecture with weak inter-network coupling, representing a resting equilibrium where inter-network coupling is minimal before the task onset.

For the emotion task, the Mid-outbound phase marks a transition from segregation to integration, initiated by visual network engagement. The Peak phase reveals task-specific reconfiguration: shape matching involves focal coupling between Visual and Dorsal Attention networks, whereas face processing triggers widespread integration of Salience and Control networks. This divergence coincides with strong deactivation of the Default Mode Network (DMN). Finally, the Mid-return phase captures the gradual restoration of baseline dynamics. Reflecting hemodynamic latency and continuous state transitions, task-evoked integration dissipates slowly, confirming the return trajectory as a relaxation process.

Similarly, the motor task displays a consistent macro-scale pattern. The Mid-outbound phase involves progressive visual-motor coupling. At the Peak, the network converges into a highly integrated state dominated by Visual, Dorsal Attention, and Somatomotor networks, facilitating the translation of visual cues into motor execution.

Importantly, while global integration is similar across different motor conditions, the manifold resolves fine-grained somatotopy. The radial segregation (Figure 6 left) is driven by specific activated ROIs within the Somatomotor network (e.g., dorsal vs. lateral regions for foot vs. tongue), while large-scale coupling remains stable. Finally, the Mid-return phase also mirrors the gradual recovery observed in the emotion task.

In summary, the precise correspondence between these distinct functional architectures and their geometric coordinates confirms the biological validity of the manifold embedding. The observed trajectories provide a compact representation of the brain's functional dynamics. Specifically, the radial distance from the origin reflects the magnitude of network reconfiguration, spanning from the modular segregation of the resting state to the global integration of the task peak. At the same time, the direction of the trajectory encodes the specificity of network engagement. By connecting the resting baseline, the task state, and the recovery phase into a continuous framework, these results demonstrate that the low-dimensional trajectory serves as a reliable model for charac-

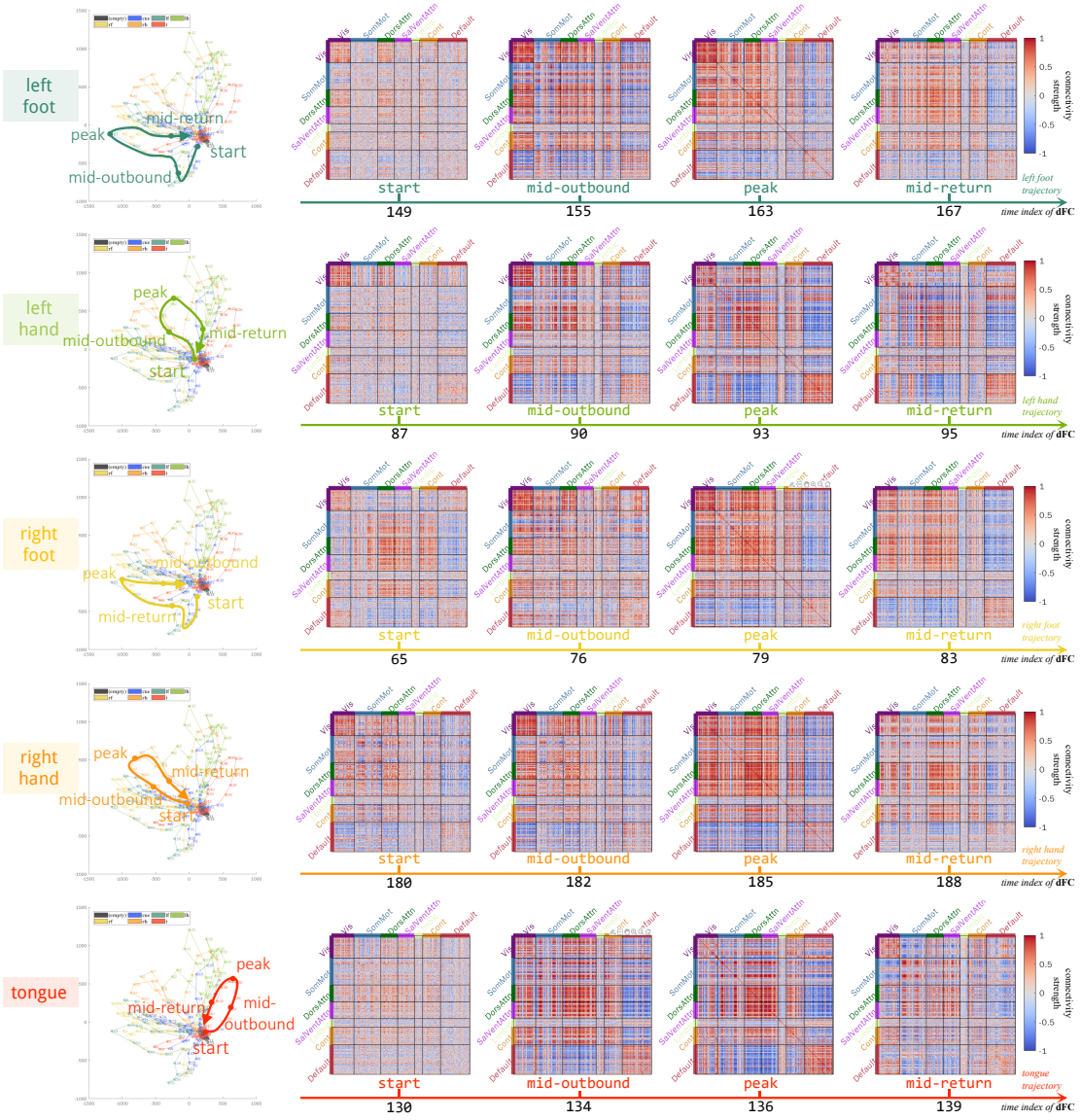

Figure 6: Looped dFC trajectories during the motor task, with representative connectivity patterns sampled at key phases along the manifold trajectory (start, mid-outbound, peak, and mid-return).

terizing the dynamic evolution of brain architecture.

Conclusion

This study introduces a geometric framework for analyzing whole-brain dynamic functional connectivity by embedding resting-state and task-evoked dynamic functional connectivity (dFC) matrices into a shared low-dimensional manifold. Within this space, brain dynamics evolve as smooth trajectories, and task engagement gives rise to structured, cyclic paths that loop away from and return to the resting-state region. These recurrent trajectories indicate continuous, reversible reconfiguration beyond discrete state transitions models. By revealing looped dFC trajectories within a unified manifold, our results highlight a stable geometric organization underlying both intrinsic activity and task-evoked modulation of large-scale brain networks. A limitation of the present work is that we rely on group-averaged dFC from two relatively simple tasks, which may obscure inter-individual variability and more complex cognitive demands. Future work will extend this manifold framework to subject-level and naturalistic paradigms, and relate trajectory geometry to behavior and clinical or cognitive phenotypes.

Acknowledgments

This work was supported by National Natural Science Foundation of China (grant No. 62376068, U24A20340, 32361143787), by Guangdong Basic and Applied Basic Research Foundation (grant No. 2023B1515120065).

References

Allen, E. A., Damaraju, E., Plis, S. M., Erhardt, E. B., Eichele, T., & Calhoun, V. D. (2014). Tracking whole-brain connectivity dynamics in the resting state. *Cerebral Cortex*, *24*(3), 663–676.

Biswal, B., Yetkin, F. Z., Haughton, V. M., & Hyde, J. S. (1995). Functional connectivity in the motor cortex of resting human brain using echo-planar mri. *Magnetic Resonance in Medicine*, *34*(4), 537–541.

Buckner, R. L., Krienen, F. M., Castellanos, A., Diaz, J. C., & Yeo, B. T. (2011). The organization of the human cerebellum estimated by intrinsic functional connectivity. *Journal of Neurophysiology*, *106*(5), 2322–2345.

Busch, E. L., Huang, J., Benz, A., Wallenstein, T., Lajoie, G., Wolf, G., Krishnaswamy, S., & Turk-Browne, N. B. (2023). Multi-view manifold learning of human brain-state trajectories. *Nature computational science*, *3*(3), 240–253.

Cohen, J. R. (2018). The behavioral and cognitive relevance of time-varying, dynamic changes in functional connectivity. *NeuroImage*, *180*, 515–525.

Gallego, J. A., Perich, M. G., Miller, L. E., & Solla, S. A. (2017). Neural manifolds for the control of movement. *Neuron*, *94*(5), 978–984.

Gao, S., Mishne, G., & Scheinost, D. (2020). Non-linear manifold learning in fmri uncovers a low-dimensional space of brain dynamics. *bioRxiv*, 2020–11.

Glasser, M. F., Coalson, T. S., Bijsterbosch, J. D., Harrison, S. J., Harms, M. P., Anticevic, A., Van Essen, D. C., & Smith, S. M. (2018). Using temporal ica to selectively remove global noise while preserving global signal in functional mri data. *Neuroimage*, *181*, 692–717.

Glasser, M. F., Coalson, T. S., Bijsterbosch, J. D., Harrison, S. J., Harms, M. P., Anticevic, A., Van Essen, D. C., & Smith, S. M. (2019). Classification of temporal ica components for separating global noise from fmri data: Reply to power. *Neuroimage*, *197*, 435–438.

Hariri, A. R., Tessitore, A., Mattay, V. S., Fera, F., & Weinberger, D. R. (2002). The amygdala response to emotional stimuli: A comparison of faces and scenes. *NeuroImage*, *17*(1), 317–323.

Huang, Z., Cai, H., Dan, T., Lin, Y., Laurienti, P., & Wu, G. (2021). Detecting brain state changes by geometric deep learning of functional dynamics on riemannian manifold. *International Conference on Medical Image Computing and Computer-Assisted Intervention*, 543–552.

Hutchison, R. M., Womelsdorf, T., Allen, E. A., Bandettini, P. A., Calhoun, V. D., et al. (2013). Dynamic functional connectivity: Promise, issues, and interpretations. *NeuroImage*, *80*, 360–378.

Logothetis, N. K. (2008). What we can do and what we cannot do with fmri. *Nature*, *453*(7197), 869–878.

Lurie, D. J., Kessler, D., Bassett, D. S., Betzel, R. F., Breakspear, M., Kheilholz, S., Kucyi, A., Liégeois, R., Lindquist, M. A., McIntosh, A. R., et al. (2020). Questions and controversies in the study of time-varying functional connectivity in resting fmri. *Network neuroscience*, *4*(1), 30–69.

Margulies, D. S., Ghosh, S. S., Goulas, A., Falkiewicz, M., Huntenburg, J. M., Langs, G., Bezgin, G., Eickhoff, S. B., Castellanos, F. X., Petrides, M., et al. (2016). Situating the default-mode network along a principal gradient of macroscale cortical organization. *Proceedings of the National Academy of Sciences*, *113*(44), 12574–12579.

Perl, Y. S., Geli, S., Pérez-Ordoyo, E., Zonca, L., Idesis, S., Vohryzek, J., Jirsa, V. K., Kringelbach, M. L., Tagliazucchi, E., & Deco, G. (2025). Modelling low-dimensional interacting brain networks reveals organising principle in human cognition. *Network Neuroscience*, *9*(2), 661–681.

Preti, M. G., Bolton, T. A., & Van De Ville, D. (2017). The dynamic functional connectome: State-of-the-art and perspectives. *NeuroImage*, *160*, 41–54.

Roberts, J. A., Gollo, L. L., Abeysuriya, R. G., Roberts, G., Mitchell, P. B., Woolrich, M. W., & Breakspear, M. (2019). Metastable brain waves. *Nature communications*, *10*(1), 1056.

Rué-Queralt, J., Stevner, A., Tagliazucchi, E., Laufs, H., Kringelbach, M. L., Deco, G., & Atasoy, S. (2021). Decoding brain states on the intrinsic manifold of human brain dynamics across wakefulness and sleep. *Communications biology*, *4*(1), 854.

Schaefer, A., Kong, R., Gordon, E. M., Laumann, T. O., Zuo, X.-N., Holmes, A. J., Eickhoff, S. B., & Yeo, B. T. (2018). Local-global parcellation of the human cerebral cortex from intrinsic functional connectivity mri. *Cerebral cortex*, *28*(9), 3095–3114.

Shine, J. M., Hearne, L. J., Breakspear, M., Hwang, K., Müller, E. J., Sporns, O., Poldrack, R. A., Mattingley, J. B., & Cocchi, L. (2019). The low-dimensional neural architecture of cognitive complexity is related to activity in medial thalamic nuclei. *Neuron*, *104*(5), 849–855.

Smith, S. M., Beckmann, C. F., Andersson, J., Auerbach, E. J., Bijsterbosch, J., Douaud, G., Duff, E., Feinberg, D. A., Griffanti, L., Harms, M. P., et al. (2013). Resting-state fmri in the human connectome project. *NeuroImage*, *80*, 144–168.

Soleimani, N., Iraji, A., van Erp, T. G., Belger, A., & Calhoun, V. D. (2025). *A method for estimating dynamic functional network connectivity gradients (dfngs) from ica captures smooth inter-network modulation* (tech. rep.). Wiley Online Library.

Tenenbaum, J. B., Silva, V. d., & Langford, J. C. (2000). A global geometric framework for nonlinear dimensionality reduction. *science*, *290*(5500), 2319–2323.

Van Essen, D. C., Smith, S. M., Barch, D. M., Behrens, T. E., Yacoub, E., Ugurbil, K., Consortium, W.-M. H., et al. (2013). The wu-minn human connectome project: An overview. *NeuroImage*, *80*, 62–79.

Vidaurre, D., Smith, S. M., & Woolrich, M. W. (2017). Brain network dynamics are hierarchically organized in time. *Pro-*

ceedings of the National Academy of Sciences, *114*(48), 12827–12832.

Yang, Y., Wang, L., Lei, Y., Zhu, Y., & Shen, H. (2019). Manifold learning of dynamic functional connectivity reliably identifies functionally consistent coupling patterns in human brains. *Brain Sciences*, *9*(11), 309.

Yeo, B. T., Krienen, F. M., Sepulcre, J., Sabuncu, M. R., Lashkari, D., Hollinshead, M., Roffman, J. L., Smoller, J. W., Zöllei, L., Polimeni, J. R., et al. (2011). The organization of the human cerebral cortex estimated by intrinsic functional connectivity. *Journal of neurophysiology*.